Study of the low-lying electronic states of CCO by photoelectron spectroscopy of CCO^- and *ab initio* calculations

V. Zengin, B. Joakim Persson,[a] K. M. Strong, and R. E. Continetti
Department of Chemistry and Biochemistry, University of California at San Diego, La Jolla, California 92093-0314

(Received 19 July 1996; accepted 3 September 1996)

The low-lying electronic states of CCO have been investigated by photoelectron spectroscopy of CCO^- at wavelengths of 266 and 355 nm in conjunction with *ab initio* calculations. Photodetachment is observed to occur to the $\tilde{X}\,^3\Sigma^-$, $\tilde{A}\,^3\Pi$, $\tilde{a}\,^1\Delta$, and $\tilde{b}\,^1\Sigma^+$ electronic states of CCO. This marks the first observation of the low-lying singlet states. A revised value for the electron affinity of CCO is found to be 2.289 ± 0.018 eV. These results are compared with CASPT2 *ab initio* calculations of the energetics and structure of the ground and excited states of CCO and CCO^-. Using the measured electron affinity of CCO, the heats of formation $\Delta_f H^0_{298}(CCO)=3.99\pm0.20$ eV and $\Delta_f H^0_{298}(CCO^-)=1.67\pm0.20$ eV are determined. In addition, the C–C bond dissociation energies in CCO and CCO^- are determined, as well as the H–CCO bond energy in HCCO. © *1996 American Institute of Physics.* [S0021-9606(96)00546-6]

I. INTRODUCTION

Ketenylidene, CCO, is known to be an important intermediate in a variety of chemical processes including hydrocarbon combustion,[1–3] molecular cloud formation in interstellar space[4,5] and the photolysis and reactions of carbon suboxide, C_3O_2.[6,7] Due to uncertainties in the thermochemistry of both CCO and CCO^-, studies of the energetics and dynamics of these molecules are of continued interest. Photoelectron spectroscopy of negative ions provides a powerful method for studying the structure and energetics of both negative ions and the corresponding neutral molecules produced by photodetachment.[8] In this paper, we report a study of CCO^- and CCO using negative ion photoelectron spectroscopy and high-level *ab initio* calculations. This work provides a new value for the electron affinity of CCO and has resulted in the first observation of the two low-lying singlet states of CCO.

The ground and excited triplet states of CCO have been previously studied spectroscopically. Matrix-isolation studies of CCO by Jacox *et al.*,[9] showed that CCO is an asymmetric linear molecule. A broad absorption was also observed near 500 nm which was tentatively assigned to photodissociation of $CCO(\tilde{X}\,^3\Sigma^-)$. In a study of CO chemiluminescence produced in the reaction of O atoms with CCO, Becker and Bayes[2] determined the heat of formation for CCO to be 4.0 ± 0.2 eV. Devillers and Ramsay[10] studied the absorption spectrum of CCO in the gas phase, observing the $\tilde{A}\,^3\Pi\leftarrow\tilde{X}\,^3\Sigma^-$ transition. Analysis of the rovibronic spectra determined the term energy (T_0) of the $\tilde{A}\,^3\Pi$ state to be 1.444 eV. In addition, vibrational frequencies, rotational constants and the Renner–Teller coupling constant for the $\tilde{A}\,^3\Pi$ state were determined.

These earlier spectroscopic studies have been followed more recently by laser induced fluorescence (LIF) studies of the kinetics, spectroscopy, and dynamics of CCO. Donnelly *et al.*[11] have measured the absolute reaction rates of $CCO(\tilde{X}\,^3\Sigma^-)$ with several small molecules using LIF. Pitts *et al.*[12] examined LIF from the $\tilde{A}\,^3\Pi$ state and calculated vibronic energy levels for both the $\tilde{A}\,^3\Pi$ and $\tilde{X}\,^3\Sigma^-$ states. This work determined a value for v_1 in the $\tilde{X}\,^3\Sigma^-$ state of 1967 cm^{-1}. Pitts *et al.*[13] and Becker *et al.*[14] studied the excited state dynamics of $CCO(\tilde{A}\,^3\Pi)$ by fluorescence and collisional quenching measurements. Most recently, a high-resolution microwave spectroscopy study by Ohshima and Endo has confirmed the structure of the ground state of CCO.[15]

The CCO^- anion has been the subject of comparatively few experimental studies. The photoelectron spectrum of CCO^- was reported by Oakes *et al.*[16] They measured the electron affinity (EA_{CCO}) to be 1.848 ± 0.025 eV, and assigned a $^2\Pi$ symmetry to the ground state of the anion using generalized valence bond (GVB) molecular orbital considerations.[17] Van Doren *et al.*[18] have studied the reactivity of CCO^- in the gas phase by selected-ion-flow drift tube and mass spectrometry, inferring significant thermodynamic information on CCO^-.

The first detailed *ab initio* study of CCO was performed by Walch.[19] Using generalized valence bond (GVB) wave functions and polarization-configuration-interaction (POL-CI) calculations, the structure and energetics of the $\tilde{X}\,^3\Sigma^-$, $\tilde{a}\,^1\Delta$, $\tilde{b}\,^1\Sigma^+$, $\tilde{A}\,^3\Pi$, and $\tilde{c}\,^1\Pi$ states were determined. These results indicated a bond dissociation energy D_0(C–CO) and heat of formation $\Delta_f H^0_0$(CCO) of 2.34 ± 0.04 eV and 3.86 ± 0.04 eV, respectively. Suter *et al.*[20] have performed multireference configuration interaction calculations of the geometry and vibrational frequencies of CCO, CNN, and NCN in their triplet ground states. The only previous theoretical study of CCO^- was performed by DeKock *et al.*[21] They calculated the geometry of both ground state CCO^- and CCO, using the complete-active-space-self-consistent-field (CASSCF) technique. No further calcula-

[a]Mailing address: San Diego Supercomputer Center, P.O. Box 85608, San Diego, California 92186-9784.

 0021-9606/96/105(22)/9740/8/$10.00

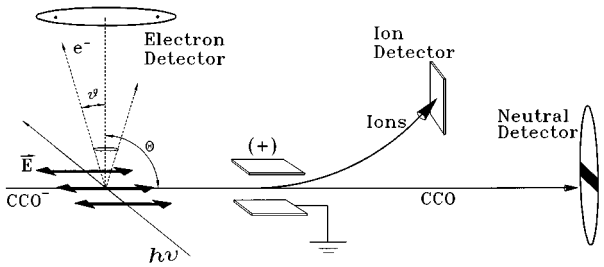

FIG. 1. Schematic of the experimental geometry. Here, Θ (denoted as laser polarization angle) is the angle between the electric vector of the laser and the nominal electron detection axis and ϑ is actual electron recoil angle with respect to the nominal electron detection axis.

tions of excited electronic states for either species have been reported.

The goal of the present study is to determine the energetics of the low-lying electronic states of CCO, using photoelectron spectroscopy of CCO^- in conjunction with high-level *ab initio* calculations. In the following section the experimental technique is reviewed, followed by a description of the complete-active-space-second-order-perturbation-theory (CASPT2) *ab initio* calculations of the low-lying states of both CCO and CCO^-. The experimental results are then presented and a Franck–Condon analysis is applied to compare the photoelectron spectra with the theoretical calculations. Finally, the implications of these studies on the energetics of CCO and CCO^- are presented.

II. EXPERIMENT

The fast-ion-beam photoelectron spectrometer used in these experiments has been previously described in detail.[22,23] A schematic of the experimental geometry is shown in Fig. 1. For the studies reported here, the photoelectron spectrometer is operated in a straight time-of-flight (TOF) mode. A mass-selected beam of CCO^- at an energy of 4 keV is crossed with a linearly polarized frequency tripled (354.8 nm, 3.494 eV) or quadrupled (266.1 nm, 4.659 eV) output of a Nd:YAG laser (Quantronix Model 116). The laser is mode-locked, Q-switched and cavity dumped at a repetition rate of 600 Hz, yielding pulses of $\sim$40 μJ/pulse at 266 nm and $\sim$60 μJ/pulse at 355 nm, with a temporal width of $\sim$100 ps FWHM.[24] The short pulsewidth of the laser has allowed reduction of the nominal field-free TOF distance for the photoelectrons from the 15 cm reported in Ref. 22 to 7.5 cm. A time- and position-sensitive detector is used to record the TOF and position-of-arrival of at most one photoelectron per laser shot. The photoelectron detector effectively subtends 4% of the solid angle about the laser interaction region. Using the time-of-flight and position of arrival, the laboratory energy and recoil angle for each photoelectron can be calculated. Measurement of the recoil angle is essential in fast-ion-beam photoelectron spectroscopy to make the large laboratory to center-of-mass frame kinematic correction produced by the velocity of the incident ion. [25] This information allows the electron kinetic energy in the center-of-mass frame (eKE) to be determined.

The photoelectron spectrometer was calibrated by photodetachment of $O^- \rightarrow O(^3P, ^1D) + e^-$ at 266 nm, giving peaks at eKE=3.198 and 1.231 eV, respectively. At 355 nm, photodetachment of O^- and I^- was used, giving peaks at 2.033 and 0.435 eV, respectively. The calibrated data reproduced these peaks with a maximum error of $\pm$0.010 eV. The nominal energy resolution $\Delta E/E$ (full-width-at-half-maximum) was determined to be $\sim$4%. The contribution of background photoelectrons from both the negative ion beam and scattered laser light is greatly mitigated by taking advantage of the heavy particle detector in our apparatus (see Fig. 1). This is done by examining only those events in which both a photoelectron and a neutral particle are produced in coincidence. Residual laser and ion beam background are measured in separate experiments and are subtracted from the data.

CCO^- was produced from carbon suboxide (C_3O_2) using a pulsed discharge ion-source.[26] The discharge was struck during the early stages of the free jet expansion, resulting in significant cooling of the ions. C_3O_2 was synthesized by the thermal decomposition of malonic acid catalyzed by phosphorous pentoxide.[27] Gaseous C_3O_2 and CO_2 were collected in a liquid nitrogen trap. This mixture was vacuum distilled twice to remove the CO_2 using an ethanol-liquid nitrogen bath at -110 °C. The C_3O_2 was stored under vacuum at dry-ice temperature (-78 °C) for days without polymeriza-

TABLE I. CASPT2 equilibrium bond lengths (Å), harmonic stretching frequencies (cm^{-1}), force constants (mdyn/Å^2), and excitation energies (eV) for CCO and CCO^-.

State	R_{CC}	R_{CO}	ω_1	ω_3	k_{11}	k_{33}	T_e	T_0
			CCO					
$\tilde{c}\,^1\Pi$	1.250	1.232	2002	1203	13.1	8.9	2.65	2.66[a]
$\tilde{A}\,^3\Pi$	1.281	1.192	2100	1270	13.9	10.2	1.30	1.34[b]
$\tilde{b}\,^1\Sigma^+$	1.366	1.186	2022	1066	14.7	6.3	1.00	1.00[a]
$\tilde{a}\,^1\Delta$	1.370	1.180	2005	1067	14.6	6.3	0.63	0.63[a]
$\tilde{X}\,^3\Sigma^-$	1.373	1.169	2038	1055	15.5	5.9	0.0	0.0
			CCO^-					
$\tilde{A}\,^2\Sigma^+$	1.261	1.244	2218	1190	13.3	10.4	1.39	1.42[a]
$\tilde{X}\,^2\Pi$	1.317	1.230	1912	1130	11.2	8.3	0.0	0.0

[a]Zero-point correction neglecting any change in ω_2.
[b]Using experimental values for ω_2 from Ref. 10.

TABLE II. Calculated and experimental equilibrium bond distances and harmonic stretching frequencies for diatomic fragments (in Å and cm^{-1}).

	Calc.		Expt.[a]	
	R_e	ω_e	R_e	ω_e
CO ($^1\Sigma^+$)	1.139	2127	1.128	2170
C_2 ($^1\Sigma_g^+$)	1.259	1840	1.243	1855
C_2^-($^2\Sigma_g^+$)	1.284	1760	1.268	1781

[a]K. P. Huber and G. Herzberg, *Molecular Spectra and Molecular Structure IV. Constants of Diatomic Molecules* (Van Nostrand Reinhold, New York, 1979).

TABLE III. Summary of thermodynamic quantities determined in this work. All energies are in eV.

System	CASPT2 ΔE	CASPT2 $+\Delta$ZPE	Literature	Expt.
$CCO(^3\Sigma^-)\rightarrow C(^3P)+CO(^1\Sigma^+)$	2.40	2.30[a]		
$CCO^-(^2\Pi)\rightarrow C(^3P)+CO(^1\Sigma^+)+e^-$	4.62	4.51[b]		
$C_2^-(^2\Sigma_g^+)\rightarrow C_2(^1\Sigma_g^+)+e^-$	3.07	3.08	3.27[c]	
$CCO^-(^2\Pi)\rightarrow CCO(^3\Sigma^-)+e^-$	2.22[d]	2.22[a,b]	1.848[e]	2.289
$O^-(^2P)\rightarrow O(^3P)+e^-$	1.36	⋯	1.46[f]	
$C^-(^4S)\rightarrow C(^3P)+e^-$	1.07		1.26[f]	

[a]Using experimental ω_2 for CCO from Ref. 9.
[b]Using an estimated ω_2=450 cm^{-1} for CCO^- ion.
[c]K. M. Ervin and W. C. Lineberger, J. Phys. Chem. **95**, 1167 (1991).
[d]CCSD(T), $4s3p2d1f$ basis 2.19 eV.
[e]Reference 16.
[f]Reference 25.

tion. The sample was then introduced into the ion source using a 4:1 mixture of CO_2+N_2O as a carrier gas at ~1 atm backing pressure. The temperature of the sample container was maintained at −40 °C during data acquisition.

III. *AB INITIO* CALCULATIONS ON CCO AND CCO^-

To provide a more complete set of theoretical predictions for both the anion and the neutral excited states, we have performed *ab initio* calculations. In order to select an electronic structure method for this work, we first note that some of the molecular species involved have a strong multiconfigurational character and cannot be expected to be well described by any method based on a single SCF reference configuration. Unfortunately, even using a small basis (such as Dunning's cc-pVDZ basis[28]) the most accurate multiconfigurational method, the multireference configuration interaction (MRCI) method, will be computationally much too expensive. We have therefore performed our *ab initio* calculations with the recently developed CASPT2 approach, which is a second-order multiconfigurational perturbation theory based on the complete active space self-consistent field (CASSCF) wave function. This method has been used on a variety of systems over the last few years, and has proven to be both reliable and accurate.[29] It is a two-step approach where the first step is to perform a CASSCF calculation including all important near-degeneracy effects and the second step is a calculation of the second-order correlation energy using the CASSCF wave function as the reference function. For a detailed discussion about the CASPT2 method we refer to the recent review article by Andersson and Roos[29] and references therein. It should be noted, however, that the original implementation was biased towards open-shell structures and systematically underestimated the energy for electron pairing processes by 3–6 kcal/mol. Andersson[30] suggested alternative zeroth-order Hamiltonians which remedied this problem, and in this work we have used the zeroth-order Hamiltonian labeled g_1 by Andersson.

There is currently no CASPT2 gradient program available so the geometry optimizations have been performed by grid-based fits. Some of the triatomic states are Renner–Teller cases[31] and it is not straightforward to calculate the bending frequencies. Since no bending vibrations are observed in these experiments, we have not attempted to calculate these. Thus only two parameters are needed for the grids, R_{CC} and R_{CO}. For each of the states of the triatomic species a CASSCF minimum was located using the DALTON program,[32] which has a second-order MCSCF geometry optimizer, and a smaller Dunning cc-pVDZ basis.[28] A grid of six points, the vertices and midpoints of a triangle with the side 0.05 a_0, was placed around the CASSCF minimum and a quadratic polynomial was fit to the CASPT2 energies for these points. The minimum of this polynomial was used as the center point for a new grid and the process was repeated until the grid was centered around the CASPT2 minimum, and the geometry converged to 10^{-4} a_0. Vibrational frequencies and force constants for the harmonic stretching modes were calculated from the fitted potential functions (see Table I). The diatomic fragments of CCO have been optimized using successive quadratic three-point fits in $1/R$ with a spacing of 0.005 a_0. The results for the diatomic fragments are shown in Table II. In this case the convergence criteria was agreement to three decimal places between the grid midpoint and the minimum of the fitted function.

The CASSCF active space consisted of the full valence space minus the oxygen $2s$ orbital which was held inactive, giving 12 active electrons in 11 orbitals. All but the $1s$ electrons were correlated in the CASPT2 calculation. In the correlated calculations, the basis sets of Widmark *et al.*[33] were used. These basis sets are atomic natural orbital (ANO) type contractions[34] of a $14s9p4d3f$ primitive set. It should be noted that the anion is included in the averaging procedure of Widmark *et al.* and these basis sets are therefore well-suited for a balanced treatment of both CCO and CCO^-. The geometry optimizations, and thus the calculations of harmonic frequencies and force constants, were performed with the $[4s3p2d1f]$ contraction. Using these geometries the energetics were recalculated with the $[5s4p3d2f]$ contraction. The CASSCF/CASPT2 calculations were performed with the MOLCAS-3 software.[35] A summary of the energetics is given in Tables I and III.

Since the ground states of CCO and CCO^- are strongly dominated by the SCF configuration, we have for comparison calculated the geometries and frequencies for these states with the $4s3p2d1f$ basis using the restricted open-shell coupled cluster [RCCSD(T)] method. These calculations were performed with the MOLPRO96 software.[36] These results

TABLE IV. Comparison between molecular parameters calculated with CASPT2 and RCCSD(T) methods (units as in Table I).

State	Method	R_{CC}	R_{CO}	ω_1	ω_3	k_{11}	k_{33}
CCO $\widetilde{X}\,^3\Sigma^-$	CASPT2	1.373	1.169	2038	1055	15.5	5.9
CCO $\widetilde{X}\,^3\Sigma^-$	CCSD(T)	1.378	1.166	2057	1058	15.8	6.0
CCO^- $\widetilde{X}\,^2\Pi$	CASPT2	1.317	1.230	1912	1130	11.2	8.3
CCO $\widetilde{X}\,^2\Pi$	CCSD(T)	1.318	1.226	1932	1134	11.4	8.4

are compared in Table IV, and show that for the ground states the two methods agree.

The most complete previous theoretical study of the ground and excited states of CCO is the work of Walch.[19] As noted in the Introduction, Walch studied the ground and low-lying states of CCO using the POL-CI method based on the generalized-valence-bond wave functions. A comparison of these results is shown in Table V. Walch's calculations for the energy of the $\widetilde{A}$ state is closer to the experimental value than the CASPT2 result. It should be noted, however, that the POL-CI method does not take dynamical correlation into account and this agreement with experiment must be considered fortuitous. The POL-CI results are systematically high by as much as 0.55 eV for the singlet excited states and also predict the ordering of the $\widetilde{b}$ and $\widetilde{A}$ states to be reversed. The CASPT2 calculations for the singlet states are within 0.03 eV of the experimental values. The CASPT2 calculation also gives an electron affinity of CCO only 0.07 eV lower than the measured value.

The calculated geometries of the $\widetilde{X}\,^3\Sigma^-$ and $\widetilde{A}\,^3\Pi$ states can be compared with those determined spectroscopically by Devillers and Ramsay.[10] They found the end-to-end bond lengths R_{CCO} for the $\widetilde{X}$ and $\widetilde{A}$ states to be ~2.52 Å and ~2.45 Å, respectively. Comparison with the CASPT2 calculations in Table I shows the theoretical bond lengths to be 0.02 Å longer than these spectroscopic measurements. In the following section the current experimental results are presented and compared with the CASPT2 calculations.

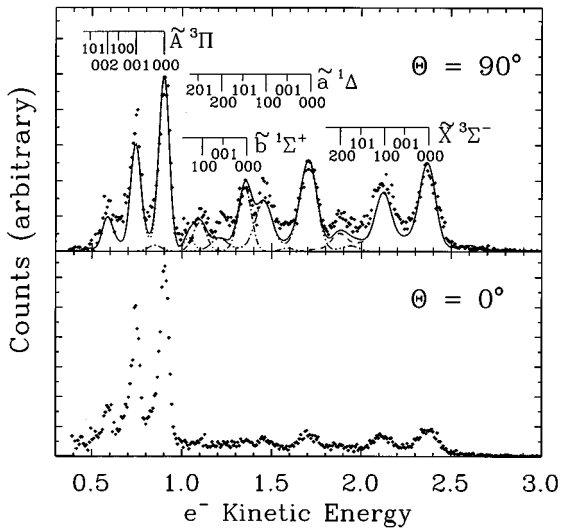

FIG. 2. Photoelectron spectrum of CCO^- at 266 nm. (Top frame) Laser polarization angle $\Theta=90°$ (see Fig. 1); (bottom frame) laser polarization angle $\Theta=0°$. The peak assignments are given by the annotated combs in the top frame. The solid line is the Franck–Condon simulation using the CASPT2 results. The dashed, dotted, and dash–dotted lines are contributions from the individual transitions. The normalization of the data in the two frames are arbitrary.

IV. PHOTOELECTRON SPECTRA OF CCO^- AND COMPARISON TO *AB INITIO* CALCULATIONS

The photoelectron spectra of CCO^- at 266 nm and 355 nm are shown in Figs. 2 and 3, respectively. The spectral assignments are also presented in Table VI. Four electronic states $\widetilde{X}\,^3\Sigma^-$, $\widetilde{a}^1\Delta$, $\widetilde{b}\,\Sigma^+$, and $\widetilde{A}\,^3\Pi$ are assigned in the spectrum at 266 nm (see Fig. 2), by comparison with previous experiments[9,10,12] and the calculations described in Sec. III. The polarization dependence of the data was studied by rotating the electric vector of the laser. As the spectra in Fig. 2 show, photoelectron signal from transitions to the $\widetilde{A}$ state is enhanced relative to the other states when the E vector is parallel to the electron detection direction ($\Theta=0°$). The $\widetilde{X}$, $\widetilde{a}$, and $\widetilde{b}$ states are also observed at 355 nm. Observation of the previously characterized $\widetilde{X}$ and $\widetilde{A}$ states of CCO in the 266 nm spectrum, with the known energy difference of 1.444 eV (Refs. 10, 12) gives a high degree of reliability to the electron affinity of CCO determined from these measurements. This separation is found to be 1.468 eV in the 266 nm spectrum in Fig. 2. The 0.024 eV difference from the previous spectroscopic determinations may arise from nonlinearities in the eKE calibration. The $\widetilde{A}$ state origin at eKE=0.900 eV is outside the range of the O^- calibration at 266 nm

TABLE V. Experimental and theoretical term energies in eV, relative to CCO $\widetilde{X}\,^3\Sigma^-(000)$.

	State	POL-CI[a] T_e	CASPT2[b] T_0	Current expt. T_0
CCO	$\widetilde{A}\,^3\Pi$	1.49	1.34	1.468 (1.444)[c]
	$\widetilde{b}\,^1\Sigma^+$	1.58	1.00	1.015
	$\widetilde{a}\,^1\Delta$	0.95	0.63	0.658
	$\widetilde{X}\,^3\Sigma^-$	0.000	0.000	0.000
CCO^-	$\widetilde{A}\,^2\Sigma^+$	⋯	−0.70	⋯
	$\widetilde{X}\,^2\Pi$	⋯	−2.22	−2.289

[a]Calculations of Walch *et al.* (Ref. 19), note that these values are T_e, with no ZPE correction.

[b]Current CASPT2 calculations including zero point energy (ZPE) correction.

[c]High-resolution spectroscopic value from Devillers *et al.* (Ref. 10).

TABLE VI. Photoelectron spectrum assignments. All values are the centroid of the peaks in the electron kinetic energy spectrum (eV).

266.0 nm	354.8 nm	State ($\nu_1\nu_2\nu_3$)
0.595	⋯	$\widetilde{A}\,^3\Pi$ (002)
0.741	⋯	$\widetilde{A}\,^3\Pi$ (001)
0.900	⋯	$\widetilde{A}\,^3\Pi$ (000)
1.098	⋯	$\widetilde{b}\,^1\Sigma^+$ (100)
1.239		$\widetilde{a}\,^1\Delta$ (200)
1.360	0.192	$\widetilde{b}\,^1\Sigma^+$ (000)
1.459	0.302	$\widetilde{a}\,^1\Delta$ (100)
1.705	0.544	$\widetilde{a}\,^1\Delta$ (000)
1.894	0.714	$\widetilde{X}\,^3\Sigma^-$ (200)
2.120	0.954	$\widetilde{X}\,^3\Sigma^-$ (100)
2.368	1.203	$\widetilde{X}\,^3\Sigma^-$ (000)

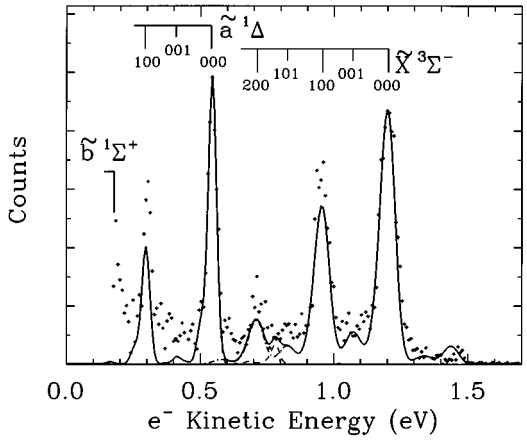

FIG. 3. Photoelectron spectrum of CCO^- at 355 nm, laser polarization angle $\Theta=90°$. The peak assignments are given by the annotated combs. The solid line is the Franck–Condon simulation using the CASPT2 results. The dashed and dash–dotted lines are contributions from the individual transitions. The $\widetilde{b}$ state is not fit since only the origin peak appears at this wavelength.

(1.231–3.198 eV). In light of this discrepancy we adopt a more conservative stated uncertainty of ±0.015 eV in all peak positions.

The origin of the $CCO(\widetilde{X}\,^3\Sigma^-)\leftarrow CCO^-(\widetilde{X}\,^2\Pi)$ progression is identified as the peaks at 2.368±0.015 eV at 266 nm and 1.208±0.015 eV at 355 nm. From the following relation:

$$EA_{CCO}=h\nu-eKE-E^0_{ion}+E^0_{neutral}, \tag{1}$$

the raw EA's of 2.291±0.015 eV and 2.286±0.015 eV, respectively, are determined. In Eq. (1), eKE is the measured electron kinetic energy corresponding to the transition CCO $\widetilde{X}\,^3\Sigma^-(000)\leftarrow CCO^-\ X\,^2\Pi(000)$ in each photoelectron spectrum. E^0_{ion} and $E^0_{neutral}$ represent the internal energy of the molecule before and after photodetachment, and are assumed to be negligible for this transition. The raw EA found in the well-resolved 355 nm spectrum is adopted. The raw EA must be corrected for rotational, ion spin–orbit, vibrational sequence bands and the position of the peak centroid.[37] The rotational correction and ion spin–orbit corrections are expected to be small. Following Oakes *et al.*,[16] we adopt an uncertainty of ±0.010 eV to account for these effects. The net effect of vibrational sequence bands and the location of the peak centroids was determined in the Franck–Condon simulation discussed below to be +0.003 eV at 355 nm. Thus, our best estimate of the EA is 2.289±0.018 eV.

A comparison with the CCO^- PES spectra of Oakes *et al.*[16] reveals that our assumption in neglecting the internal energy contributions to Eq. (2) is plausible. Comparison of the spectrum they recorded at 2.540 eV photon energy with the present data shows that the three highest energy peaks observed in their spectra originate from vibrationally excited CCO^-. Their measurements thus provide an experimental value of $\omega_1\sim1900$ cm^{-1} for the ground state of the anion. This is confirmed by the current CASPT2 calculations of the vibrational frequencies of CCO^- (see Table I). Weak υ_1 and υ_3 hot bands appearing in our spectra at both wavelengths are fit in the Franck–Condon simulations described below using the frequencies in Table I.

The low lying singlet states of CCO are observed in these experiments for the first time. The term energies T_0 of the $\widetilde{a}\,^1\Delta$ and $\widetilde{b}\,^1\Sigma^+$ states are determined from the Franck–Condon simulations of the spectra to be 0.658±0.018 and 1.015±0.018 eV, respectively, as listed in Table V. The T_0 results from the current CASPT2 calculations, shown in Table V, are in good agreement with the measured values. The frequencies for the normal mode ν_1 of the $\widetilde{a}$ and $\widetilde{b}$ states are determined to be 1950±170 and 2010±170 cm^{-1}, respectively. These values are obtained from the spectra at 355 nm for the $\widetilde{a}$ state and at 266 nm for the $\widetilde{b}$ state.

The observed spectra can be compared with the geometries and force constants found in the *ab initio* calculations via Franck–Condon simulations.[37–39] The experimentally determined electron affinity and excitation energies of the states of CCO are used in this calculation. In addition, the simulation is normalized to the different electronic states observed in the spectrum. The experimental frequencies for ν_1 and ν_3 in the $\widetilde{X}$ and $\widetilde{A}$ states of CCO were taken from Ref. 9 and for ν_2 from Ref. 10. Given the sparse experimental information for the other states and anion as well, we adopt the theoretical calculations in Table I. The bending mode frequency of the anion is estimated to be ≈450 cm^{-1} for the purpose of these simulations. From the calculated changes in the individual bond lengths and the force constants in the various electronic states, (in Table I), the changes in normal coordinates may be found using the Wilson FG matrix method.[37] The changes in the normal coordinates and bond distances, summarized in Table VII, are used to calculate Franck–Condon factors for the normal modes in each electronic state. In these calculations, we assume that the normal modes are of the same form in both the anion and the neutral, i.e., we neglect mode-mixing effects due to Duschinsky rotation.[39] In the Franck–Condon simulations, the vibrational temperature of the anion was also varied and estimated to be ~1100 K for the ν_1, ν_3 modes, and 800 K for ν_2, based on the weak hot bands and sequence band effects on the observed peak shapes at 355 nm.

The Franck–Condon simulations using the CASPT2 re-

TABLE VII. Normal coordinate analysis of the CCO^- photoelectron spectrum using CASPT2 geometries and force constants. The Δr_i and ΔR_{CCO} are in units of Å and defined as (neutral)-(anion). The normal coordinate changes ΔQ_i are in units of Å(amu)$^{1/2}$.

Final state (CCO)	Δr_{CC}	Δr_{CO}	ΔR_{CCO}	ΔQ_1	ΔQ_3
$\tilde{X}\ ^3\Sigma^-$	+0.056	−0.061	−0.005	+0.152	−0.078
$\tilde{a}\ ^1\Delta$	+0.053	−0.050	+0.003	+0.141	−0.046
$\tilde{b}\ ^1\Sigma^+$	+0.049	−0.044	+0.005	+0.129	−0.036
$\tilde{A}\ ^3\Pi$	−0.036	−0.038	−0.074	−0.026	−0.193

sults are shown as the fits to the data in Figs. 2 and 3. Good overall agreement between the simulation and the data are observed. The absence of resolved bending excitation in the spectra confirms that the states of the neutral and the anion are linear. The most striking observation in the spectra is that photodetachment produces ν_1 excitation in transitions to the $\tilde{X}$, $\tilde{a}$, and $\tilde{b}$ states and ν_3 excitation in transitions to the $\tilde{A}$ state. This provides an important test of the *ab initio* calculations, and as the simulation shows, this change is predicted. The remaining differences between the spectra and the Franck–Condon simulations in part arise from uncertainties in the subtraction of laser and ion-beam-related photoelectron background.

Further insights into the photoelectron spectra may be gained through a qualitative discussion of the electronic configurations of the observed states of CCO and CCO^-. The dominant electronic configuration of the ground state of the anion can be written as

$$\ldots(4\sigma)^2(5\sigma)^2(6\sigma)^2(1\pi)^4(7\sigma)^2(2\pi)^3\ \ \tilde{X}\ ^2\Pi. \tag{2}$$

Removal of an electron from the highest-occupied $(2\pi)^3$ molecular orbital produces the following single-configuration picture of the low-lying neutral states,[40]

$$\ldots(4\sigma)^2(5\sigma)^2(6\sigma)^2(1\pi)^4(7\sigma)^2(2\pi)^2$$

$$\tilde{X}\ ^3\Sigma^-,\ \ \tilde{a}\ ^1\Delta,\tilde{b}\ ^1\Sigma^+, \tag{3}$$

which are the first three states observed in the photoelectron spectra. Removal of an electron from the $(7\sigma)^2$ molecular orbital produces the configuration[10]

$$\ldots(4\sigma)^2(5\sigma)^2(6\sigma)^2(1\pi)^4(7\sigma)^1(2\pi)^3\ \ \tilde{A}\ ^3\Pi,\ \ \tilde{c}\ ^1\Pi. \tag{4}$$

The $\tilde{A}\ ^3\Pi$ state is observed in these experiments.

These one-electron photodetachment schemes are in agreement with the observed laser polarization dependence of the photoelectron signal shown in Fig. 2. Photodetached electrons that correspond to production of the $\tilde{A}$ state are observed to peak along the laser electric vector. As discussed above, these electrons are expected to originate from a 7σ molecular orbital. On the other hand, photodetached electrons corresponding to production of the $\tilde{X}$, $\tilde{a}$, and $\tilde{b}$ states, derived by photodetachment from a 2π molecular orbital, are observed to peak perpendicular to the laser electric vector (see Fig. 1). A similar observation regarding the polarization dependence is mentioned by Bradforth *et al.*[37] in a study of the photodetachment of CN^-, NCO^-, and NCS^-. They observed that the angular distribution of photoelectrons removed from the highest occupied σ MO in CN^- peaks along the laser electric vector, while those originating in the highest occupied π MO's in NCO^- and NCS^- peak perpendicular to the laser electric vector.

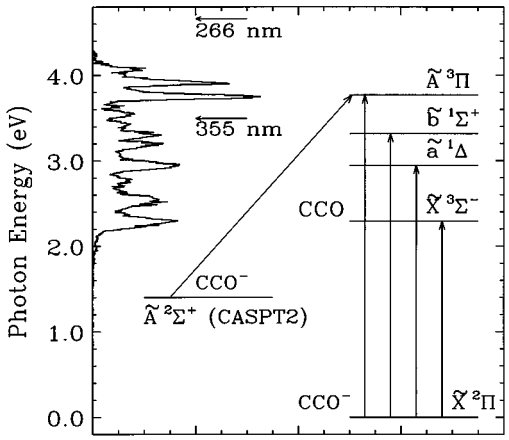

FIG. 4. Energetics diagram showing the one electron dipole-allowed transitions from CCO^- to CCO. The 266 nm photoelectron spectrum is shown on the vertical energy scale. The energy of $\tilde{A}\ ^3\Pi$ is from Ref. 10, all other energies are the term energies determined in this work. The energy of the excited anion state $\tilde{A}\ ^2\Sigma^+$ is the T_0 value determined in the current CASPT2 calculations.

Figure 4, adapted from Oakes *et al.*,[16] shows an energy level diagram for the dipole-allowed one electron transitions from CCO^- to CCO. The photoelectron spectrum recorded at 266 nm (Fig. 2) is shown on the vertical energy scale. This figure summarizes the energetics of the low-lying states of CCO as experimentally determined in the present study. As noted by Oakes *et al.*,[16] photodetachment of the excited $\tilde{A}\ ^2\Sigma^+$ state of the anion can also produce the $\tilde{A}\ ^3\Pi$ state of CCO. No evidence for this anion excited state has been observed.

V. ENERGETICS OF CCO AND CCO^-

The electron affinity of CCO experimentally determined in this study has implications for the energetics of both CCO and CCO^-. The heat of formation of CCO can be calculated as follows:

$$CCO^- \rightarrow CCO + e^-\ \ EA = 2.289 \pm 0.018\ \text{eV}, \tag{5}$$

$$HCCO \rightarrow CCO^- + H^+$$

$$\Delta H^0_{\text{acid},0} = 15.661 \pm 0.18\ \text{eV}\ \ (\text{Ref. } 18), \tag{6}$$

$$e^- + H^+ \rightarrow H\ \ -\text{IP(H)} = -13.599\ \text{eV}\ \ (\text{Ref. } 41). \tag{7}$$

Combining these three reactions yields the enthalpy of dissociation at 0 K, D_0 (H–CCO),

$$HCCO \rightarrow H + CCO\ \ D_0(\text{H–CCO}) = 4.35 \pm 0.18\ \text{eV}. \tag{8}$$

Assuming the integrated heat capacities of CCO (0.108 eV) (Ref. 41) and HCCO cancel, and given the integrated heat capacity of $H=0.064$ eV,[42] the enthalpy of dissociation $D_{298}(\mathrm{H-CCO})=4.41\pm0.18$ eV can be calculated. Now, using the previously measured $\Delta_f H^0_{298}(\mathrm{HCCO})=1.84\pm0.09$ eV[16]

$$\Delta_f H^0_{298}(\mathrm{CCO})=D_{298}(\mathrm{H-CCO})+\Delta_f H^0_{298}(\mathrm{HCCO})-\Delta_f H^0_{298}(\mathrm{H}) \quad (9)$$

which results in $\Delta_f H^0_{298}(\mathrm{CCO})=3.99\pm0.20$ eV. This value of $\Delta_f H^0_{298}(\mathrm{CCO})$ is in excellent agreement with the previous experimental value of Becker *et al.*[2] The enthalpy of dissociation $D_{298}(\mathrm{C-CO})$ can be calculated using the measured value for the $\Delta_f H^0_{298}(\mathrm{CCO})$ and values from the JANAF thermochemical tables for the heat of formation of C and CO (Ref. 41) as follows:

$$D_{298}(\mathrm{C-CO})=\Delta_f H^0_{298}(\mathrm{C})+\Delta_f H^0_{298}(\mathrm{CO})-\Delta_f H^0_{298}(\mathrm{CCO}) \quad (10)$$

which results in $D_{298}(\mathrm{C-CO})=2.29\pm0.20$ eV. This value is in good agreement with the CASPT2 calculations. Similarly, using $D_{298}(\mathrm{C-CO})$ and the electron affinities for CCO and C,[41] the enthalpy of dissociation D_{298} $(\mathrm{C^-}-\mathrm{CO})=3.31\pm0.20$ eV is determined. The heat of formation $\Delta_f H^0_{298}=1.67\pm0.20$ eV for $\mathrm{CCO^-}$ may also be calculated using the measured EA, $\Delta_f H^0_{298}(\mathrm{CCO})$ and the integrated heat capacity of the electron at 298 K, 0.0325 eV.[41] Given the importance of CCO and HCCO as combustion intermediates, these amended values for the thermodynamic parameters may be of interest to combustion modelers.

VI. CONCLUSIONS

Photoelectron spectroscopy of $\mathrm{CCO^-}$ at 266 and 355 nm has provided an improved value for the electron affinity of CCO, 2.289 ± 0.018 eV. The $\tilde{a}\,^1\Delta$ and $\tilde{b}\,^1\Sigma^+$ states of CCO have been observed in this experiment for the first time. The term energies of these states are determined to be 0.658 ± 0.018 eV and 1.015 ± 0.018 eV, respectively. These results are compared with extensive new CASPT2 calculations on the electronic structure of both CCO and $\mathrm{CCO^-}$. These calculations compare favorably with the measured electron affinity and term energies of the excited states of CCO. In addition, using the theoretical predictions, a normal coordinate analysis and Franck–Condon simulations of the photoelectron spectra were performed. Good overall agreement between theory and experiment is seen, in particular the theory correctly predicts that photodetachment of $\mathrm{CCO^-}$ yields CCO with ν_1 excitation in the ground and low-lying singlet states and ν_3 excitation in the first triplet excited state. This further verifies the utility of the CASPT2 method for the energetics and structure of the excited states of small molecules and anions. The implications of our results on the energetics of CCO and $\mathrm{CCO^-}$ are reviewed. Using the measured electron affinity of CCO and available thermodynamic data, we have determined the C–C bond dissociation energy and heat of formation for CCO and $\mathrm{CCO^-}$. In addition, we find a revised value for the H–CCO bond dissociation energy. The CASPT2 calculations indicate that the $\tilde{c}\,^1\Pi$ state is 2.66 eV above the ground state of CCO. We hope to identify and study the dissociation dynamics of this state with 213 nm laser photodetachment in the near future.

ACKNOWLEDGMENTS

This work was supported by the Chemistry Division of the National Science Foundation (CHE-9321786). R.E.C. acknowledges support from a Camille and Henry Dreyfus New Faculty Award and a 1994 Packard Fellowship in Science and Engineering. B.J.P. was supported by the National Science Foundation through Grant No. CHE-9320718 to P. R. Taylor. The electronic structure calculations were performed on either a Cray C90 or an IBM RS/6000 350 at the San Diego Supercomputer Center. We acknowledge K. A. Hanold, K. R. Mackie, and S. Winoto for their contributions to this project.

[1] K. D. Bayes, J. Chem. Phys. **52**, 1903 (1970).
[2] K. H. Becker and K. D. Bayes, J. Chem. Phys. **48**, 653 (1968).
[3] A. Fontijn and S. E. Johnson, J. Chem. Phys. **59**, 6193 (1973).
[4] M. Ohishi, H. Suzuki, S. Ishikawa, C. Yamada, H. Kanamori, W. M. Irvine, R. D. Brown, P. D. Godfrey, and N. Kaifu, Astrophys. **380**, L39 (1991).
[5] R. D. Brown, D. M. Cragg, P. D. Godfrey, W. M. Irvine, and D. McGonagle, J. Intl. Soc. Study Origin Life **21**, 399 (1992).
[6] C. Willis and K. D. Bayes, J. Am. Chem. Soc. **88**, 3202 (1967).
[7] C. E. M. Strauss, S. H. Kable, G. K. Chawla, P. L. Houston, and I. R. Burak, J. Chem. Phys. **94**, 1837 (1990).
[8] K. M. Ervin and W. C. Lineberger, in *Advances in Gas Phase Ion Chemistry*, edited by N. G. Adams and L. M. Babcock (JAI, Greenwich, 1992), Vol. 1, pp. 121–166.
[9] M. E. Jacox, D. E. Milligan, N. G. Moll, and W. E. Thomson, J. Chem. Phys. **43**, 3734 (1965).
[10] C. Devillers and D. A. Ramsay, Can. J. Phys. **49**, 2839 (1971).
[11] V. M. Donnely, W. M. Pitts, and J. R. McDonald, Chem. Phys. **49**, 289 (1980).
[12] W. M. Pitts, V. M. Donnelley, A. P. Baronavski, and J. R. McDonald, Chem. Phys. **61**, 451 (1981).
[13] W. M. Pitts, V. M. Donnelley, A. P. Baronavski, and J. R. McDonald, Chem. Phys. **61**, 465 (1981).
[14] K. H. Becker, R. König, R. Meuser, P. Wiesen, and K. D. Bayes, J. Photochem. Photobiol. A **64**, 1 (1992).
[15] Y. Ohshima and Y. Endo, J. Chem. Phys. **102**, 1493 (1994).
[16] J. M. Oakes, M. E. Jones, V. M. Bierbaum, and G. B. Ellison, J. Phys. Chem. **87**, 4810 (1983).
[17] W. A. Goddard III, T. H. Dunning, Jr., W. J. Hunt, and P. J. Hay, Acc. Chem. Res. **6**, 368 (1973).
[18] J. M. Van Doren, T. M. Miller, A. E. Stevens-Miller, A. A. Viggiano, R. A. Morris, and J. F. Paulson, J. Am. Chem. Soc. **115**, 7407 (1993).
[19] S. P. Walch, J. Chem. Phys. **72**, 5679 (1980).
[20] H. U. Suter, M.-B. Huang, and B. Engels, J. Chem. Phys. **101**, 7686 (1994).
[21] R. L. DeKock, R. S. Grev, and H. F. Schaefer III, J. Chem. Phys. **89**, 3016 (1988).
[22] K. A. Hanold, C. R. Sherwood, M. C. Garner, and R. E. Continetti, Rev. Sci. Instrum. **66**, 5507 (1995).
[23] C. R. Sherwood, Ph.D. thesis, University of California, San Diego, 1995.
[24] X. Xie and J. D. Simon, Optics Commun. **69**, 303 (1989).
[25] H. Hotop and W. C. Lineberger, J. Phys. Chem. Ref. Data **14**, 731 (1985).
[26] D. L. Osborn, D. J. Leahy, D. R. Cyr, and D. M. Neumark, J. Chem. Phys. **104**, 5026 (1996).
[27] G. Brauer, *Handbook of Preparative Inorganic Chemistry*, 2nd ed. (Academic, New York, 1963), p. 648.
[28] T. H. Dunning, Jr., J. Chem. Phys. **90**, 1007 (1989).
[29] K. Andersson and B. O. Roos, in *Modern Electronic Structure Theory*,

Part 1, edited by D. Yarkony (World Scientific, Singapore, 1995).
[30] K. Andersson, Theor. Chim. Acta **91**, 225 (1995).
[31] G. Herzberg, *Molecular Spectra and Molecular Structure, Vol. III Electronic Spectra and Molecular Structure of Polyatomic Molecules* (Van Nostrand, Princeton, 1966).
[32] DALTON is an electronic structure program written by T. Helgaker, H. J. Aa. Jensen, P. Jørgensen, H. Koch, J. Olsen, H. Ågren, K. L. Bak, V. Bakken, O. Christiansen, A. Halkier, P. Dahle, H. Heiberg, H. Hettema, D. Jonsson, R. Kobayashi, A. S. deMeras, K. V. Mikkelsen, P. Normann, K. Ruud, P. R. Taylor, and O. Vahtras.
[33] P.-O. Widmark, P. Å. Malmqvist, and B. O. Roos, Theor. Chim. Acta. **77**, 291 (1990).
[34] J. Almlöf and P. R. Taylor, J. Chem. Phys. **86**, 4070 (1987).
[35] K. Andersson, M. R. A. Blomberg, M. P. Fülscher, G. Karlström, V. Kellö, R. Lindh, P. Å. Malmqvist, J. Noga, J. Olsen, B. O. Roos, A. J. Sadlej, P. E. M. Siegbahn, M. Urban, P.-O. Widmark, MOLCAS-3, University of Lund, Sweden.
[36] MOLPRO96 is a package of *ab initio* programs written by H. J. Werner and P. J. Knowles with contributions from J. Almlöf, R. D. Amos, M. J. O. Deegan, S. T. Elbert, C. Hampel, W. Meyer, K. Peterson, R. Pitzer, A. J. Stone, P. R. Taylor, and R. Lind. The RCCSD method is described in P. J. Knowles, C. Hampel, and H.-J. Werner, J. Chem. Phys. **99**, 5219 (1993) and the triples (T) correction in J. D. Watts, J. Gauss, and R. J. Bartlett, J. Chem. Phys. **98**, 8718 (1993).
[37] S. E. Bradforth, E.-H. Kim, D. W. Arnold, and D. M. Neumark, J. Chem. Phys. **98**, 800 (1993).
[38] D. W. Arnold, Ph.D. thesis, University, of California, Berkeley, 1994.
[39] K. M. Ervin, J. Ho, and W. C. Lineberger, J. Phys. Chem. **92**, 5405 (1988).
[40] G. Herzberg, *The Spectra and Structure of Simple Free Radicals* (Cornell University Press, Ithaca, 1971), pp. 124–127.
[41] M. W. Chase, Jr., C. A. Davies, J. R. Downey, Jr., D. J. Frurip, R. A. McDonald, and A. N. Syverud, J. Phys. Chem. Ref. Data **14**, Suppl. 1 (1985); $\Delta_f H^0_{298}(\mathrm{CO}) = -1.146$ eV, $\Delta_f H^0_{298}(\mathrm{C}) = 7.428$ eV, $\mathrm{EA(C)} = 1.263$ eV, $H_0 - H_{298}$ (CCO) $= 0.108$ eV.
[42] J. E. Bartmess, J. Phys. Chem. **98**, 6423 (1994).